

Mars Reconnaissance Orbiter Ka-Band Carrier Signal Analysis

David D. Morabito*

ABSTRACT — This article reports on the Ka-band (32 GHz) signal strength data acquired during the Mars Reconnaissance Orbiter (MRO) cruise phase between November 2005 and February 2006, which occurred shortly after launch. Earlier reports focused on MRO performance with respect to various requirements involving telemetry and navigation, such as testing different modulation and coding schemes, different pointing techniques, as well as evaluating differential one-way ranging (DOR), Doppler and ranging performance. For this study, the received carrier-to-noise density P_c/N_0 measurements were adjusted to a standard range distance of 1 astronomical unit (AU) and a carrier-only mode so that the measurements from different tracking passes can be easily compared. The P_c/N_0 measurements from four Deep Space Network (DSN) 34-m diameter Ka-band capable antennas were compared against favorable and adverse link budget curves as a function of elevation angle. We compiled and compared the statistics of the adjusted MRO P_c/N_0 measurements with analyses from other Ka-band missions. The adjusted P_c/N_0 signal level statistics acquired from tracking data over these multiple missions were integrated, consolidated, and distilled. This resulted in discerning a recommended link margin that would be useful in the early planning stages of missions considering or planning to use Ka-band. By employing a 4-dB margin relative to adverse link assumptions, a project can expect to achieve at least 95 percent data return. The margin can be reduced (or tightened) as knowledge of link budget parameters improves.

I. Introduction

Ka-band (32 GHz) offers several advantages over lower frequency bands, such as wider spectrum allocation, higher antenna gain, and greater immunity to plasma effects. These advantages facilitate increased telemetry performance and greater accuracy for differential one-way ranging (DOR), Doppler, and ranging navigation data types. Early deep-space Ka-band experiments and demonstration flights included Mars Observer, Mars Global Surveyor, Deep Space 1, and Mars Reconnaissance Orbiter (MRO). More recent Ka-band missions whose signal strength data have been analyzed include Cassini [1], Kepler [2], and Lunar Reconnaissance Orbiter (LRO) [3]. The focus of this study was on revisiting the MRO Ka-band carrier data in the context of performing a statistical analysis in the same manner

* Communications Architectures and Research Section.

as was done previously for Cassini [1] and Kepler [2] and to integrate these results into the overall Ka-band statistical database.

The MRO spacecraft was launched on August 12, 2005 and inserted into Mars orbit on March 10, 2006. Between these two events, MRO had an active Ka-band campaign during early cruise lasting from late 2005 to early 2006 [4–11]. Among the highlights for MRO was achieving the highest Ka-band data rate ever from a planetary mission, 6 Mbps, which was limited by spacecraft hardware. During cruise, the MRO Ka-band link possessed extra margin that allowed for a complete evaluation of telemetry performance [6]. In addition, radiometric data in the form of Doppler and ranging acquired by MRO along with differential one-way ranging (DOR) at Ka-band were evaluated and compared with the concurrent X-band (8.4 GHz) results [8]. A follow-up study discussed the performance of Ka-band radiometric observables after they had been folded into navigation solutions of spacecraft state vectors [5]. In addition, the results of several DOR experiments involving MRO Ka-band were also documented [11].

MRO presented challenges not normally associated with planetary missions. This was primarily because of the high level of signal power received at the ground stations during early cruise as the MRO-to-Earth distance was relatively small. In addition, the spacecraft transmitted the Ka-band signal over the high-gain antenna (HGA) at these short distances, since Ka-band could only be used with this antenna. The resulting high level of received signal power caused problems with obtaining accurate measurement of the in-flight equivalent isotropic radiated power (EIRP) of the spacecraft, as there were saturation problems with the ground receiver. This made it difficult to accurately measure received signal power as the receiver was operating in a non-linear region. The initial signal-to-noise measurements acquired during the first Ka-band pass at Deep Space Station 25 (DSS-25, which is a 34-m antenna at Goldstone, California) were much lower than expected. As a result, DSS-13 (a research and development 34-m beam waveguide [BWG] antenna located at Goldstone, California) was utilized in an attempt to accurately measure spacecraft EIRP [7]. Given that the initial measurements at DSS-13 indicated that spacecraft EIRP was 5 dB below pre-launch measurements, the MRO project was requested to leave the Ka-band signal turned on in carrier-only mode for most of the cruise phase [9]. The DSS-13 campaign led to the development and exercise of strong-signal EIRP measurement techniques useful for future high-power deep-space missions [7]. Because of the saturation issues, several of the earlier passes during cruise were rendered useless for accessing P_c/N_0 statistical behavior. There were also some issues with establishing adequate pointing such as with DSS-25 in Goldstone, California. However, active pointing [12] and blind pointing of the Deep Space Network's (DSN's) other operational BWG antennas used in the demonstration (DSS-26, DSS-34, and DSS-55 discussed later in this article) performed reasonably well.

More recently, a significant quantity of deep-space Ka-band observations from the Cassini and Kepler missions was analyzed to statistically infer atmospheric effects such as those due to attenuation and noise temperature increase. The Ka-band carrier data acquired at all three DSN tracking sites (Goldstone, California; Madrid, Spain; and Canberra, Australia) were examined in order to characterize link performance over a wide range of weather conditions and as a function of elevation angle. A comprehensive study of the Cassini

carrier signal strength data involved ~2 million closed-loop (1-s) observations acquired over ~10 years [1]. Based on this analysis, we derived a baseline Ka-band link margin that flight projects may consider in preflight planning. Here an adverse threshold assumption of 90 percent weather availability and a margin of 4 dB (relative to adverse assumptions) were derived to cover our perception of increased uncertainties at the 32-GHz Ka-band link frequency. It was found that a 4-dB margin below adverse assumptions will ensure a ~95 percent data return at a minimum 20-deg elevation angle under 90 percent weather conditions at 32-GHz Ka-band. Given that this margin should in practice yield over 99 percent data return due to atmospheric effects alone, it is expected that there is likely “slop” due to other loss effects such as due to unknown residual pointing errors that may lie in the 1 to 2 dB range. This conclusion was reinforced based on follow-up analysis of several years of Kepler Ka-band data [2].

During the MRO Ka-band demonstration, the distance between the spacecraft and Earth varied from 0.098 astronomical unit (AU) on September 24, 2005 (2005-267) to 1.03 AU on February 1, 2006 (2006-033). For easy comparison of P_c/N_0 measurements between passes, all of the measurements were adjusted to a common range distance of 1 AU. In addition, since numerous coding schemes, modulation schemes, and modulation indices were exercised for MRO at Ka-band, the P_c/N_0 measurements were adjusted to the common carrier-only mode, by backing out the appropriate suppression values to the P_c/N_0 measurements that were used for telemetry, ranging and DOR. This allowed for an equitable comparison of the data over the different configurations.

We will discuss recommendations for projects with regard to Ka-band margin policy and thresholds. We focused on the adverse link curves using them as a boundary from which we infer the number of measurements that lie below these curves. We inspected potential margin values relative to the adverse link curves versus the respective fraction of the acquired data lying above the margin curves for each tracking site. This was done with the intent of identifying a reasonable margin that would provide an acceptable loss fraction as a baseline recommendation. Flight projects can then use these results as one consideration in their criteria. Individual flight projects may utilize margins that are larger or smaller as their link design evolves depending on evolution of link budget uncertainties and mission phase.

Section II provides a discussion on the results acquired from the DSS-25 and DSS-26 DSN stations at Goldstone, California (II.A.), the DSS-34 station at Canberra, Australia (II.B.), and the DSS-55 station at Madrid, Spain (II.C.). Section III provides discussion on the integration and combining of the MRO signal strength statistics with those from Cassini and Kepler, as well as distillation of the results in a manner useful to those mission managers and telecom engineers using or considering Ka-band for present and future missions.

II. Observations

The performance behavior of the Ka-band carrier power-to-noise density measurements (P_c/N_0) acquired at the three DSN sites (at Goldstone, California; Canberra, Australia; and Madrid, Spain) will be discussed. In order to compare measurements acquired at different

range distances and different telemetry/ranging modes, we have adjusted all of the measurements to a common range distance of 1 astronomical unit (AU), and a common on-board downlink mode of carrier only. Thus, we made use of known telemetry, ranging, and DOR modulation suppressions to perform the adjustments.

A. P_c/N_0 Ka-Band Analysis for Goldstone, California

The Ka-band downlink P_c/N_0 measurements (adjusted) acquired from the two 34-m diameter BWG antennas (DSS-25 and DSS-26) at Goldstone, California were examined.

A review of the MRO Cruise Report (CR)¹ showed that the received signal strength measurements from several of the DSS-25 passes were not usable, even though they all had adequate margin to realize many of the demonstration objectives involving the exercise of different modulation and coding schemes such as for telemetry. In this report, all subsequent references to the MRO Cruise Report will use the notation “(CR)”. Most of the DSS-25 passes were plagued by high losses of a non-atmospheric origin and thus were removed from statistical consideration of the received P_c/N_0 statistics. The DSS-25 passes occurred on the following “year-day of year” designations: 2005-267, 2005-280, 2005-315, 2005-319, 2005-322, 2005-323, 2005-324, 2005-344, 2005-354 and 2005-359. Based on the previous MRO studies (which focused on analyzing Ka-band telemetry and navigation performance), there were several equipment-related issues, rendering most of the DSS-25 passes unusable for this purpose. The blind pointing model at DSS-25 was not yet fully developed, and its use resulted in large variations in the received signal strength measurements. In addition, the monopulse active pointing correction system at DSS-25 was not yet fully operational during these early set of passes between September 24 and November 30, 2005.

Figure 1 displays the adjusted P_c/N_0 for the best two DSS-25 passes (2005-344 and 2005-354) that were considered. The data points for individual passes are color-coded as noted in the legend. Also plotted are the favorable link curve (black), adverse link curve (red) and “Adverse – 4 dB” link curve (dashed yellow). Virtually all of the data points lie below the favorable link curve (black) which assumes 50 percent weather, with the highest P_c/N_0 values hugging the lower edge of this curve. The adverse link budget curve (red) lies about 1–2 dB below the favorable curve accounting for 90 percent weather for both attenuation in P_c , and added atmospheric noise temperature in N_0 . For consistency with previous studies [1 and 2], we plotted the “Adverse – 4 dB” curve. Ideally, less than 1 percent of the data should lie below this curve. As seen in Figure 1, a significant amount of data lie below this curve.

Upon close inspection of the P_c/N_0 versus time series for pass 2005-354 (Figure 1 green points), we see that the peaks of the data points lie close to the 72 dB-Hz favorable link limit; however, there are numerous dropouts that extend as far as 10 to 12 dB down. The DOR segments (green dashes between ~18- and ~36-deg elevation angles), appear to be very stable but are about 6 dB down even after the known 12.04 dB suppression

¹ S. Shambayati, MRO Ka-band Demonstration Cruise Activities Report, Rev. A, JPL D-31190 (internal document), Jet Propulsion Laboratory, California Institute of Technology, Pasadena, California, April 9, 2007.

adjustment for DOR is applied. This also appears to be the case with the 2005-344 DOR segments seen in Figure 1 (gray dashes between 15 and 34 deg elevation).

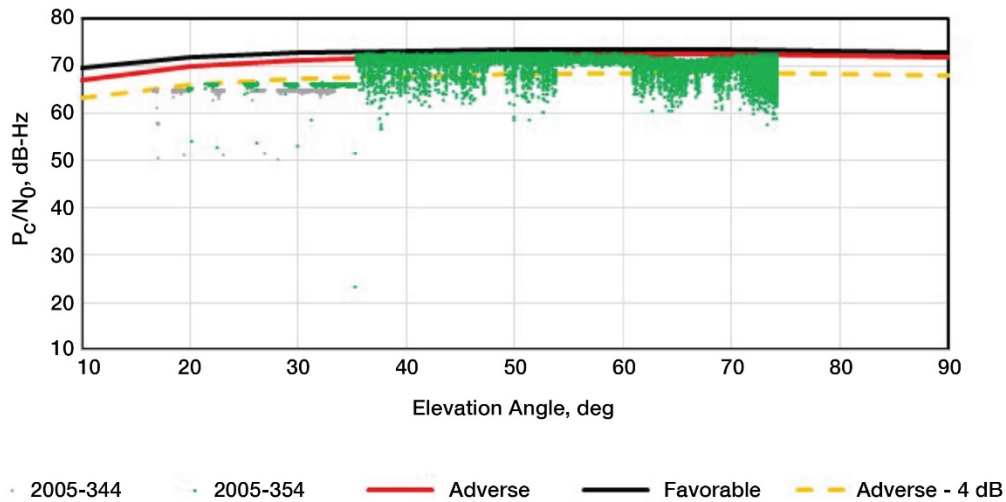


Figure 1. Adjusted P_c/N_0 versus elevation angle for selected passes at DSS-25 (colored points), favorable link curve (black), adverse link curve (red), and “Adverse – 4 dB” link curve (dashed yellow).

Most of the problems with the low dropouts for passes earlier than 2005-344 appear to be related to issues with strong uplink and low modulation index (CR). Thus, data from pass 2005-315 were not used even though weather did contribute to visible degradation.

In any event, given that there are issues with all of the DSS-25 passes during the Ka-band demonstration, we chose not to include any of this data for the overall analysis. Thus, it is emphasized that the shortfall of P_c/N_0 such as shown in Figure 1 is unique to DSS-25 at the time of the MRO Ka-band demonstration, and it is not indicative of general Ka-band performance.

The DSS-26 34-m diameter BWG antenna at Goldstone was also used to acquire downlink Ka-band data for several MRO cruise passes. Several of the initial passes during the demonstration were plagued by pointing problems and thus were not usable for characterizing atmospheric (and other “unknown”) effects on the P_c/N_0 observables. These passes occurred on days 2005-320, 2005-336, 2005-361, 2005-362, 2006-001, 2006-003, and 2006-011. The various issues associated with these P_c/N_0 measurements are discussed in detail in the Cruise Report (CR) and in the literature [4–11]. The data from several of the later demonstration passes were deemed successful as the received signal power decreased to manageable levels as the range distance increased.

Starting on 2006-014, the pointing issues were resolved, and the quality of the data from DSS-26 was vastly improved. Figure 2 displays the adjusted P_c/N_0 for DSS-26 after removal of data associated with known pointing deficiencies and other issues. The data points for individual passes are identified in the legend. Also plotted are the favorable link curve (black), the adverse link curve (red) and the “Adverse – 4 dB” link curve (dashed yellow). Note that virtually all of the data points lie near the favorable link curve (black) which assumes 50 percent weather, with the highest P_c/N_0 values hugging this curve for elevation

angles greater than 40 deg. The adverse link budget curve (red) lies about 1 to 2 dB below the favorable curve accounting for 90 percent weather for both attenuation in P_c , and added atmospheric noise temperature in N_0 . For consistency with previous studies, we also plotted the “Adverse – 4 dB” curve. Ideally, less than 1 percent of the data should lie below this curve. As can be seen from Figure 2, a small amount of the data does lie below this curve.

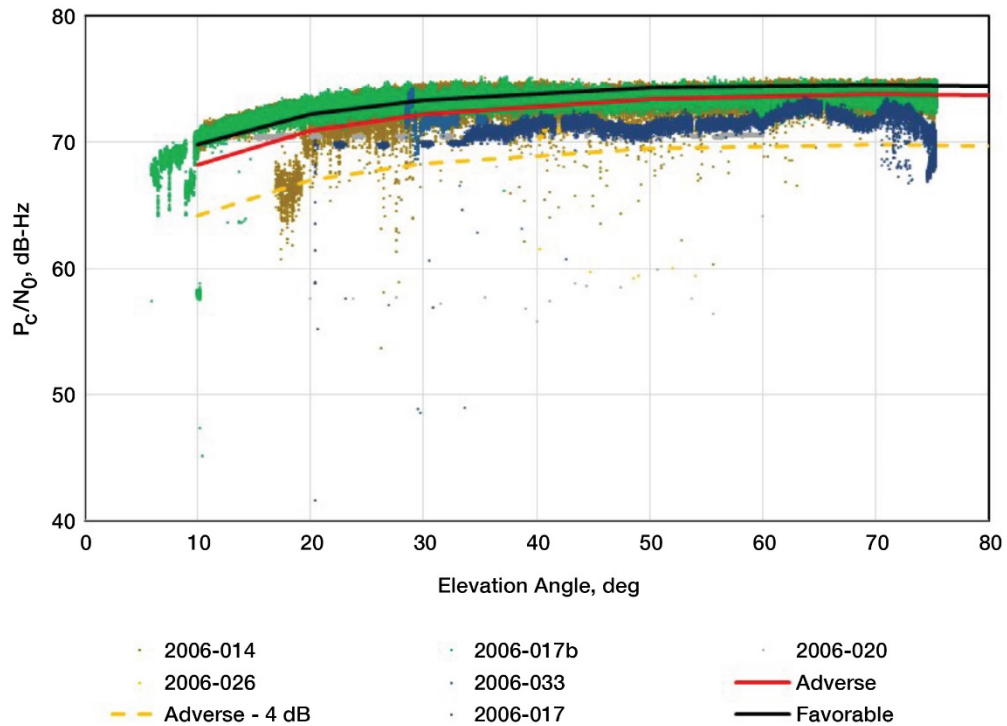


Figure 2. Adjusted P_c/N_0 versus elevation angle for data acquired at DSS-26 (colored points) along with favorable link curve (black), adverse link curve (red), and “Adverse – 4 dB” link curve (dashed yellow).

Table 1 displays the statistics for the data for each DSS-26 pass plotted in Figure 2, showing pass ID, approximate start and stop times in Coordinated Universal Time (UTC), the total number of data points plotted, and the total number of data points that lie above the “Adverse – 4 dB” curve (dashed yellow). The final column shows the percent of data lying above this curve. Ideally, we expect better than 99 percent of the data to lie above this curve, which is what we see for most of the listed passes. The overall percentage of DSS-26 data lying above the “Adverse – 4 dB” curve is about 98 percent.

We chose not to include data from pass 2006-011 in the overall statistical characterization given in Figure 2 and Table 1. Figure 3 displays the time series of the adjusted P_c/N_0 (blue data points) from pass 2006-011, the “Adverse – 4 dB” curve (dashed yellow), the system noise temperature (SNT) from the closed-loop system (yellow data points), and SNT derived from local zenith advanced water vapor radiometer (AWVR) 31.4-GHz zenith brightness temperature data adjusted for elevation angle (red data points). The SNT from the DSS-26 receiving equipment and the SNT derived from the nearby AWVR are in excellent agreement, and these signatures support the conclusion that weather is not a

factor in the large adjusted P_c/N_0 excursions seen to lie below the “Adverse – 4 dB” curve. It appears that many of the P_c/N_0 data points fall below the “Adverse – 4 dB” curve, such as the large variations seen during the first half of the pass where the blind pointing model is known to be deficient (CR). The monopulse-derived pointing errors (from adjacent passes) were shown to be large in this portion of the sky during the first (rising) half of the passes where this pointing system was used. We conclude that losses due to the blind pointing for this pass are likely responsible for reduction of the P_c/N_0 and given that it is difficult to adjust for any mispointing, we chose not to include the data from this pass in the overall statistical characterization of DSS-26 Ka-band as already provided in Table 1.

Table 1 – DSS-26 passes used in statistical study.

Pass ID	UTC Start	UTC End	Total Number of Points	Number > 4 dB Curve	Percent > 4 dB Curve
2006-014	21:09	9:10	42,055	41,702	99.2
2006-017	2:00	8:02	16,889	15,225	90.1
2006-017b	20:25	8:50	45,363	45,267	99.8
2006-020	20:54	0:37	4,312	4,293	99.6
2006-026	22:46	0:07	2,312	2,305	99.7
2006-033	21:34	22:47	2,043	2,016	98.7
Totals			112,974	110,808	98.1

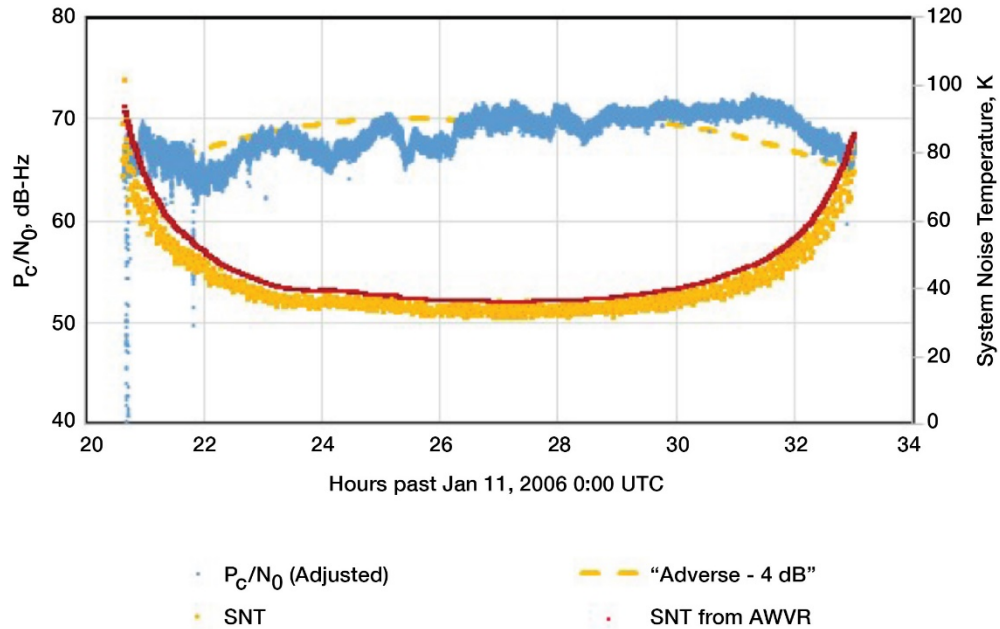


Figure 3. Adjusted P_c/N_0 (blue points) for 2006-011 along with SNT measured at DSS-26 (yellow points), SNT derived from AWVR data (red points), and the “Adverse – 4dB” curve (dashed yellow curve) versus UTC time.

The P_c/N_0 data for passes 2006-017b and 2006-014 lie on or just below the “Favorable Link” curve in Figure 2, consistent with the model when the pointing and weather are good. We

see from Figure 4 that for pass 2006-014, even with the periodic signal drops due to range interference, almost all of the P_c/N_0 data points lie above the “Adverse – 4 dB” curve. We chose to retain the data from these two passes in the statistical study.

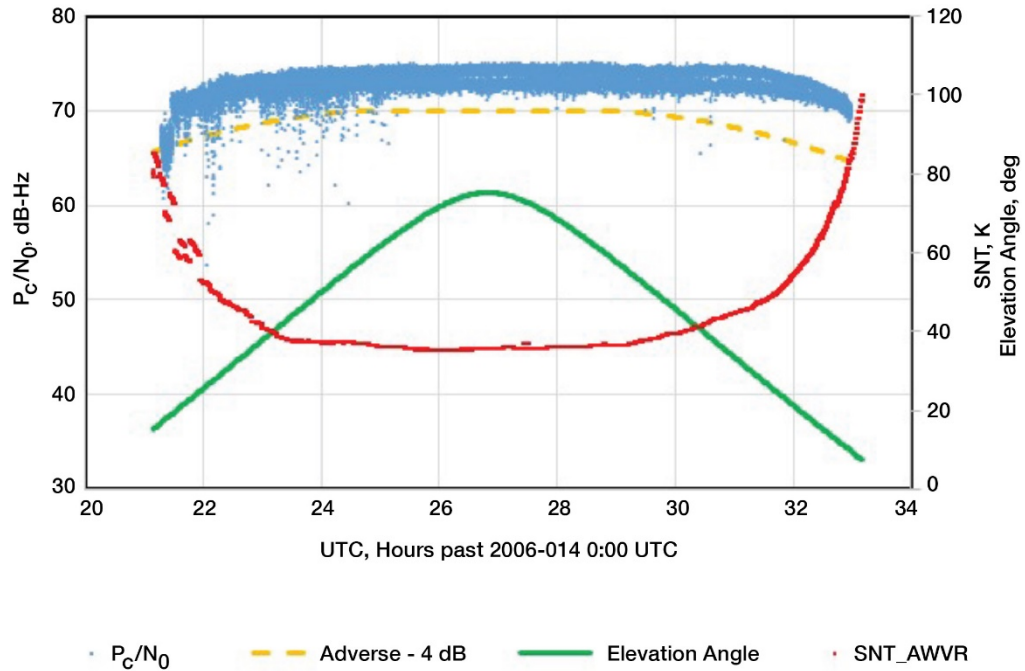


Figure 4. Adjusted P_c/N_0 (blue data points), SNT derived from AWVR (red data points), elevation angle (solid green), and “Adverse – 4 dB” curve (dashed yellow) for pass 2006-014.

From the results of Table 1, we see that about 98 percent of the data lie above the “Adverse – 4 dB” curve which is in reasonable agreement with the results of the previous studies [1–2] (see also Sec. III).

B. P_c/N_0 Ka-band Analysis for Canberra, Australia

Due to the high declination of the spacecraft during the MRO Ka-band demonstration, the peak elevation angle for the Southern Hemisphere Canberra, Australia DSN site did not exceed 36 deg. Data from DSS-34 is most reliable because the spacecraft does not get as high in elevation as it does for the other stations and DSS-34 has better blind pointing model (CR). About 11 tracking passes were conducted. Five of these passes were deemed unusable and were conducted on 2005-290, 2005-318, 2005-344, 2005-353 and 2005-354. The details of the problems associated with these passes are discussed in the MRO Cruise Report (CR) and literature [4–11].

The adjusted Ka-band P_c/N_0 data for six passes not plagued by pointing or other non-weather problems are shown in Figure 5 as a function of elevation angle. As can be seen from Figure 5, almost all of the P_c/N_0 observations lie above the “Adverse – 4 dB” curve, even with the 3-dB “drops” due to ranging interference seen in some passes. Table 2 provides a statistical summary of the data from the usable passes plotted in Figure 5.

Table 2 – DSS-34 passes used in statistical study.

Pass ID	Start Time UTC	End Time UTC	Total Number of Points	Number of Pts. > 4 dB	Percent > 4 dB Curve
2005-319	8:10	15:45	24,799	24,743	99.77
2005-360	7:30	14:05	17,092	17,037	99.68
2005-361	9:25	14:05	14,639	14,638	99.99
2005-363	7:35	13:55	18,441	18,434	99.96
2006-001	7:35	13:55	19,072	19,038	99.82
2006-002	8:00	13:35	26,238	26,238	100.00
Totals			120,281	120,128	99.90

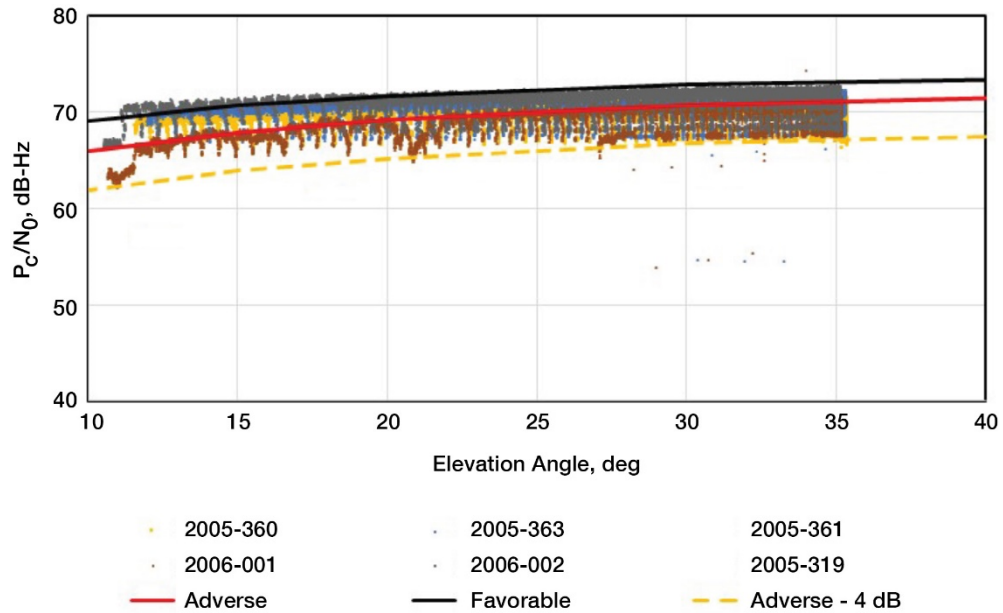


Figure 5. Adjusted P_c/N_0 versus elevation angle for data acquired at DSS-34 (colored points) along with favorable link curve (black), adverse link curve (red), and “Adverse – 4 dB” link curve (dashed yellow).

As just stated, almost all of the data plotted in Figure 5 lie above the “Adverse – 4 dB” curve, with the lower portions of the P_c/N_0 signatures just touching this curve. For instance, pass 2006-001 exhibits these “drops” every ranging cycle as shown in Figure 6, but with almost all data lying above the “Adverse – 4 dB” curve. This peculiar phenomenon, indicative of interference from the ranging tones, occurred during several cruise demonstration passes with details provided in the MRO Cruise Report (CR) and literature [9].

The symbol signal-to-noise ratio (SSNR or E_s/N_0) values for pass 2006-001 reported for the Ka-band telemetry channel are, in general, within 0.5 dB of predicts [CR]. However, there is a 6 dB drop in the SSNR towards the end of the pass. This is probably due to the weather as the weather data indicate high humidity and later rain during the day, and this is substantiated by the high SNT measurements shown in Figure 6. In addition, there is a high incidence of weather-related effects shown in the SNT at the start of the pass, where some of this effect is apparent in the DOR segments between 07:00 and 08:30 UTC. In any

event, virtually all of the data, (even with the 3 dB-down-ranging interference) lie above the 4-dB down curve; and thus, this provides an example where we can include these data in the statistics (as shown in Table 2) without instituting complicated adjustment schemes or intensive “hand editing” removal of these data points.

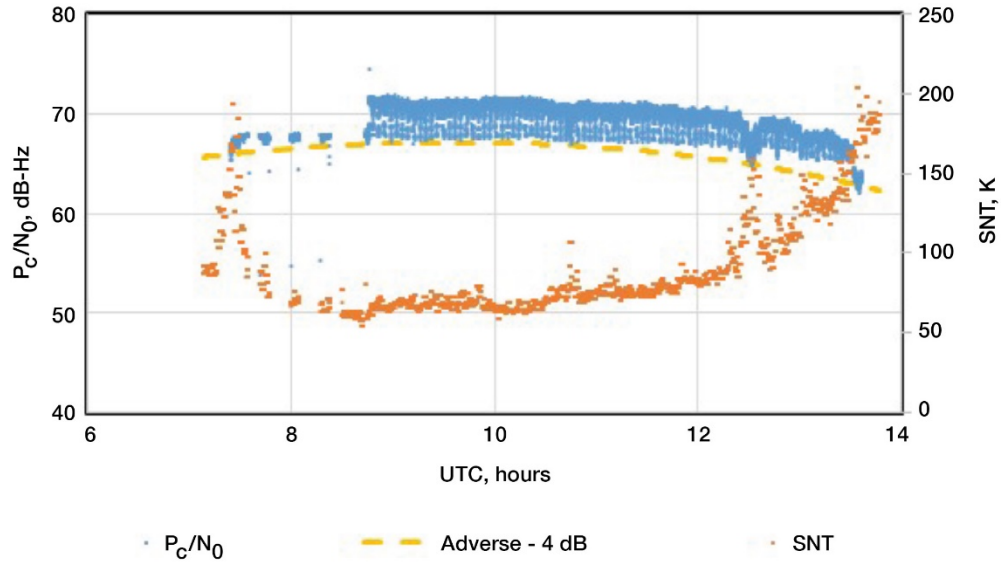


Figure 6. Adjusted P_c/N_0 (blue) for pass 2006-001 along with “Adverse – 4 dB” curve (dashed yellow) and SNT measured at DSS-34 (brown) versus UTC time.

For the remaining DSS-34 passes shown in Figure 5, it appears that almost all of the data lie above the “Adverse – 4 dB” curve (dashed yellow), including the range interference points. This is numerically reflected in Table 2 showing about 99.9 percent of the data lie above this curve. Given that we are bookkeeping statistics of the data that lie above and below the 4-dB curve, and virtually all of the bottoms of the range point dips lie above this curve, it was deemed unnecessary to attempt any “corrections” of the range dips or removal of these data.

C. P_c/N_0 Ka-band Analysis for Madrid, Spain

There were 14 tracking passes conducted at DSS-55 with seven passes being deemed unusable and include 2005-304, 2005-319, 2005-320, 2005-323, 2005-324, 2005-325 and 2005-339. Although many of these passes realized many of objectives of the MRO Ka-band demonstration given their high margins, they were removed from this study due to issues with mostly pointing and other non-atmospheric effects, as they occurred very early during periods of strong-signal saturation issues. Details are described in the MRO CR and elsewhere in the literature [4–11].

Figure 7 displays adjusted P_c/N_0 for seven tracking passes conducted at DSS-55 in Madrid, Spain during MRO early cruise in which the data were deemed usable for the statistical study. Table 3 lists the passes for which the P_c/N_0 data were used in the analysis along with the start and stop times and relevant statistics. Note that from Table 3 about 95 percent of

the data seen in Figure 7 lie above the “Adverse – 4 dB” curve. We expect that there may be some pointing issues and selection effects on order of 1 to 2 dB. The bottoms of range interference dips may also be skewing these results such as seen between 45 and 70 deg elevation angle in Figure 7. Thus, it is understood that some of the data lying below the “Adverse – 4 dB” curve in Figure 7 includes some “skewing” due to non-atmospheric effects. We thus consider 95 percent as a conservative estimate, as any attempt to “filter” out these data would result in a somewhat higher percentage above 95 percent.

Table 3 – DSS-55 passes used in statistical study.

Pass ID	Start Time UTC	End Time UTC	Total Number of Points	Number of Pts. > 4 dB	Percent > 4 dB Curve
2005-362	13:40	0:00	31,603	29,803	94.3
2005-364	13:35	2:00	42,479	40,615	95.6
2006-001	13:25	0:40	26,659	25,223	94.6
2006-010	21:00	1:44	12,941	12,427	96.0
2006-020	20:47	0:42	2,078	2,067	99.5
2006-026	22:38	23:58	2,208	2,201	99.7
2006-033	21:33	23:29	3,779	3,772	99.8
Totals			121,747	116,108	95.4

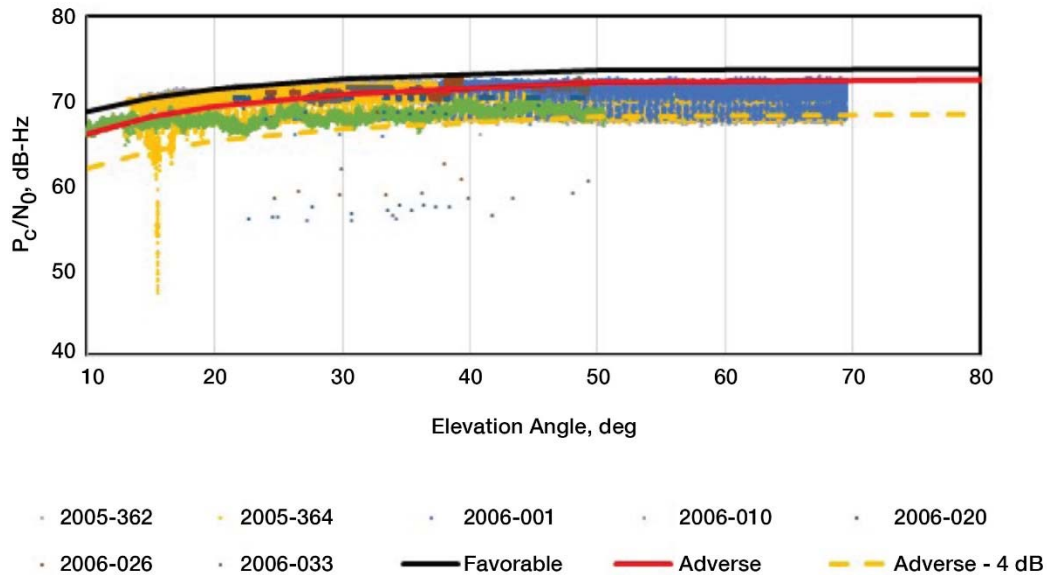


Figure 7. Adjusted P_c/N_0 versus elevation angle for data acquired at DSS-55 (colored points) along with favorable link curve (black), adverse link curve (red), and “Adverse – 4 dB” link curve (dashed yellow).

III. Discussion of Consolidated Ka-Band P_c/N_0 Statistics and Margin Policy

The Ka-band results from previous studies for Cassini [1], for Kepler [2], and from the present study for MRO have been integrated and consolidated. Table 4 incorporates the results from these three studies, in the form of percentages of adjusted P_c/N_0 measurements that lie above the “Adverse – 4 dB” link curve. We see that 98 percent of the adjusted P_c/N_0

measurements lie above this curve for Goldstone, 95 percent for Madrid and 97 percent for Canberra. Thus, by employing a 4-dB margin below adverse link assumptions, one can realize at least a 95 percent success rate in data acquisition,² where there are contributions due to uncorrected mispointing (or other unknown effects) in addition to the atmosphere.

Table 4 –Summary of deep space Ka-band P_c/N_0 measurements.

Goldstone				
	Number of Obs	Number Obs > 4 dB Curve	Percent > 4 dB Curve	
Cassini	730,922	715,738	97.92	See Note (1)
Kepler	131,108	124,889	95.26	See Note (2)
MRO	112,974	110,808	98.08	See Note (3)
Total	975,004	951,435	97.58	

Madrid				
	Number of Obs	Number Obs > 4 dB Curve	Percent > 4 dB Curve	
Cassini	832,745	785,738	94.36	See Note (1)
Kepler	142,101	139,751	98.35	See Note (2)
MRO	121,747	116,108	95.37	See Note (3)
Total	1,096,593	1,041,597	94.98	

Canberra				
	Number of Obs	Number Obs > 4 dB Curve	Percent > 4 dB Curve	
Cassini	527,328	512,100	97.11	See Note (1)
Kepler	86,793	83,362	96.05	See Note (2)
MRO	120,281	120,128	99.87	See Note (3)
Total	734,402	715,590	97.44	

- Notes:
- (1) From Cassini Study [1]
 - (2) From Kepler Study [2]
 - (3) MRO (this study) Nov 2005–Feb 2006

The results depicted in Table 4 have been filtered by the removal of data from tracking passes with obvious equipment issues including many with conspicuous pointing losses as previously discussed. The remaining data utilized in this analysis includes smaller but unknown effects including pointing loss that may reach the 1 to 2 dB range. Ideally, if the atmosphere is the only unadjusted effect, the success rate should be greater than 99

² We assume that the margin discussion relating to the carrier channel can easily be applicable to the telemetry data channel assuming appropriate assumptions are made regarding modulation index, implementation loss, coding threshold, etc.

percent at the 4 dB below adverse link assumption level. Many of the data points lying below the “Adverse – 4 dB” curves are likely dominated by non-atmospheric effects. The most obvious example from the MRO results involve the Madrid data as seen from inspection of Figure 7. Given that it is difficult to model these effects out or hand delete these points, any removal of these points from consideration will likely change the Madrid 95 percent success rate for MRO to a somewhat higher value. Other effects that skewed the results below the 99 percent level from some passes included the effects of high winds at the Goldstone DSN site for both Cassini [1] and Kepler [2].

Since this overall study spans multiple deep-space Ka-band missions (MRO, Cassini, and Kepler), the similarity in results between flight projects provides confidence that the DSN 34-m diameter antennas behave similarly (from 94 percent to ~100 percent depending upon the selection of passes deemed usable). It should be pointed out that a similar study for near-Earth K-band (26 GHz) involving the Lunar Reconnaissance Orbiter (LRO) spacecraft in orbit around the Moon achieved a close to 99 percent success rate using the 18-m antenna at White Sands, New Mexico [3]. This was closer to expectations and suggested that the performance for both the White Sands ground antenna and/or the LRO spacecraft was somewhat better than that experienced for the DSN at Ka-band.

Table 4 thus represents the integration, consolidation, and distillation of the acquired Ka-band signal strength data from three deep-space missions, all normalized to common range distance and tracking mode. Operations managers of present and future Ka-band missions can use the Table 4 results in their planning of Ka-band operations. A 4-dB margin level below adverse assumptions provides a safe and reasonable margin to use in link budgets for future space missions that can cover other unforeseen uncertainties in link assumptions other than atmosphere, during early mission design. Ka-band missions typically will evolve their designs so that as they get closer to or reach their operational phases, their link margins will change as their knowledge of spacecraft performance evolves, as improvements in ground station tracking performance are realized, as uncertainties of non-atmospheric link effects are reduced, and as a function of mission phase. The adoption of assured delivery protocols with feedback could allow missions to operate at lower margins. Examples of such protocols include fully acknowledged Consultative Committee for Space Data Systems (CCSDS) file delivery protocol (CFDP) and disruption tolerant networking (DTN).

Acknowledgements

We would like to thank Barry Geldzahler of NASA Headquarters and Faramaz Davarian of Jet Propulsion Laboratory (JPL) for providing support for this work. We would also like to thank Julian Breidenthal of JPL for many useful review comments. We would also like to thank the MRO Telecom Team at Lockheed-Martin in Denver, Colorado for providing needed support in addressing questions that arose during this analysis. We also thank James Border at JPL for providing important information regarding the MRO DOR passes.

References

- [1] Morabito, D. D., D. Kahan, K. Oudrhiri, and C.-A. Lee, "Cassini Downlink Ka-Band Carrier Signal Analysis," *Interplanetary Network Progress Report*, vol. 42-208, Jet Propulsion Laboratory, California Institute of Technology, Pasadena, California, pp. 1–22, February 15, 2017. https://ipnpr.jpl.nasa.gov/progress_report/42-208/208B.pdf
- [2] Morabito, D. D., "Deep-Space Ka-Band Flight Experience," *Interplanetary Network Progress Report*, vol. 42-211, Jet Propulsion Laboratory, California Institute of Technology, Pasadena, California, pp. 1–16, November 15, 2017. https://ipnpr.jpl.nasa.gov/progress_report/42-211/211B.pdf
- [3] Morabito, D. D., and D. Heckman, "Lunar Reconnaissance Orbiter K-Band (26 GHz) Signal Analysis: Initial Study Results," *Interplanetary Network Progress Report*, vol. 42-211, Jet Propulsion Laboratory, California Institute of Technology, Pasadena, California, pp. 1–20, November 15, 2017. https://ipnpr.jpl.nasa.gov/progress_report/42-211/211A.pdf
- [4] Shambayati, S., D. Morabito, J. S. Border, and F. Davarian, "Mars Reconnaissance Orbiter Ka-Band Demonstration: Cruise Phase Operations," in *Space Operations: Mission Management, Technologies, and Current Applications*, edited by L. Bruca, J. P. Douglas, and T. Sorensen, *Progress in Astronautics and Aeronautics Series*, Vol. 220 AIAA, pp. 249–274, 2007.
- [5] Morabito, D. D., E. Graat, J. Border, and S. Shambayati, "Interplanetary Spacecraft Navigation Using Ka-band Radiometric Observables," *Proceedings of the 13th Ka and Broadband Communications Conference*, Turin, Italy, September 24–26, 2007.
- [6] Shambayati, S., J. S. Border, D. D. Morabito, and R. Mendoza, "MRO Ka-Band Demonstration: Cruise Phase Lessons Learned," *Proceedings of IEEE Aerospace Conference*, Big Sky, Montana, March 3–10, 2007.
- [7] Morabito, D. D., D. Lee, M. M. Franco, and S. Shambayati, "Measurement of Mars Reconnaissance Orbiter Equivalent Isotropic Radiated Power during Early Cruise," *Interplanetary Network Progress Report*, vol. 42-168, Jet Propulsion Laboratory, California Institute of Technology, pp. 1–19, February 15, 2007. https://ipnpr.jpl.nasa.gov/progress_report/42-168/168F.pdf
- [8] Morabito, D. D., Mendoza, R., Highsmith, D., Border, J., and Shambayati, S. "Analysis of Ka-band Radiometric Data Acquired during Cruise of the Mars Reconnaissance Orbiter," *Proc. of the 12th Ka and Broadband Comm. Conf.*, September 27–29, 2006 Naples, Italy. pp. 259-266.
- [9] Shambayati, S., D. Morabito, J. Border, F. Davarian, D. Lee, R. Mendoza, M. Britcliffe, and S. Weinreb, "Mars Reconnaissance Orbiter Ka-band (32 GHz) Demonstration: Cruise Phase Operations," *Proceedings of SpaceOps Conference*, Rome, Italy, American Institute of Aeronautics and Astronautics, June 23, 2006.
- [10] Shambayati, S., F. Davarian, and D. Morabito, "Link Design and Planning for Mars Reconnaissance Orbiter (MRO) Ka-band (32 GHz) Telecom Demonstration," Paper

#1383, *Proceedings of the 2005 IEEE Aerospace Conference*, Big Sky, Montana, March 2005.

- [11] Border, J. S., "A Global Approach to Delta Differential One-way Range," Paper: 2006-d-49, *Proceedings of 25th ISTS (International Symposium on Space Technology and Science) and 19th ISSFD (International Symposium on Space Flight Dynamics)*, Kanazawa, Japan, June 4–11, 2006.
- [12] Gudim, M. A., W. Gawronski, W. J. Hurd, P. R. Brown, and D.M. Strain, "Design and Performance of the Monopulse Pointing System of the DSN 34-Meter Beam-Waveguide Antennas," *The Telecommunications and Mission operations Progress Report*, April–June 1999, vol. 42-138, Jet Propulsion Laboratory, California Institute of Technology, Pasadena California, pp. 1–29, August 15, 1999.
https://ipnpr.jpl.nasa.gov/progress_report/42-138/138H.pdf

Acronyms and Terms

“Adverse – 4 dB” curve obtained by subtracting 4 dB from the adverse link curve values

AU astronomical unit

AWVR advanced water vapor radiometer

BWG beam waveguide

CFDP Consultative Committee for Space Data Systems file delivery protocol

CCSDS Consultative Committee for Space Data Systems

CR Mars Reconnaissance Orbiter Cruise Report (Footnote 1)

dB decibel

DOR differential one-way ranging

DSN Deep Space Network

DSS Deep Space Station

DSS-13 a research and development 34-m beam waveguide antenna at Goldstone, California

DSS-25 34-m beam waveguide Deep Space Station at Goldstone, California

DSS-26 34-m beam waveguide Deep Space Station at Goldstone, California

DSS-34 34-m beam waveguide Deep Space Station at Canberra, Australia

DSS-55 34-m beam waveguide Deep Space Station at Madrid, Spain

DTN disruption tolerant networking

EIRP equivalent isotropic radiated power

E_s/N_0 symbol signal-to-noise ratio (alternate to SSNR)

HGA high gain antenna

JPL	Jet Propulsion Laboratory
K-band	25.5 to 27 GHz allocation used for near-Earth downlink
Ka-band	31.8 to 32.3 GHz allocation used for deep space downlink
LRO	Lunar Reconnaissance Orbiter
MRO	Mars Reconnaissance Orbiter
P_c/N_0	received carrier-to-noise density
SNT	system noise temperature
SSNR	symbol signal-to-noise ratio
UTC	Coordinated Universal Time or Universal Time Coordinated
X-band	8.4 GHz

CL#18-3716